Report No. DOE/ER/54181-9

RENSSELAER POLYTECHNIC INSTITUTE
Non-Profit Educational Institution
Troy, New York 12180-3590

Final Technical Report

Entitled

DEVELOPMENT OF RADIATION-HARDENED CERAMIC COMPOSITES FOR FUSION APPLICATIONS

For

USDOE Grant No. DE-FG02-ER54181

for the period

1 September 2003 through 31 August 2004

Submitted on behalf of

Don Steiner
Institute Professor of Nuclear Engineering
Nuclear Engineering and Engineering Physics Program
Department of Mechanical, Aerospace, and Nuclear Engineering

INTRODUCTION

This Progress Report describes work performed as a collaborative effort between Rensselaer Polytechnic Institute (RPI) and Oak Ridge National Laboratory (ORNL). This research is focused in four areas considered to be critical issues [1] for using SiC fiber-reinforced SiC matrix composites (SiC/SiC) as structural materials in a fusion environment:

- Calculation of the critical dose and temperature for amorphization of SiC by using the TRIM computer code to analyze ORNL and literature data
- Measurement of irradiation-induced creep in monolithic SiC or stoichiometric SiC fibers
- Determining the effects of high-temperature irradiation on monolithic SiC as part of ORNL's METS experiment
- Gauging the effectiveness of polymer impregnation pyrolysis in improving SiC/SiC composite hermeticity

Progress in each area is described below, as well as plans for next year.

COMPUTER MODELING OF RADIATION DAMAGE IN SIC

The computer code TRIM [2, 3] is widely used by the fusion community to estimate damage for many types of ion beam irradiation experiments. With the recent release of TRIM-2003, work continues to:

- Calculate the amorphization threshold dose of SiC at room temperature
- Calculate the critical temperature for amorphization of SiC
- Assess the accuracy of TRIM

TRIM-2003 is a "major release" of the TRIM code. The last major release was TRIM-98, significantly updating the stopping powers used in the calculations. TRIM-2003 includes new theoretical calculations addressing the stopping of heavy ions at lower energies, which should affect the results for several of the experimental cases under analysis.

Amorphization threshold dose at room temperature is calculated by comparing experimentally observed amorphous regions with TRIM damage profiles generated for the same ion beams and fluences. As was done with TRIM-98 , TRIM-2003 is being used to update the threshold dose calculations for ORNL and literature experiments (Table 1). Calculation of the critical temperature for amorphization of SiC is being attempted in the same manner, but TRIM does not factor temperature into the calculations and the results are therefore less accurate.

The accuracy of the damage profiles produced by TRIM depends on user input, TRIM's stopping powers, and the TRIM computational code itself. Analysis continues for an eventual *Nuclear Instruments and Methods B* paper on the errors possible in calculating displacement damage values for ion-irradiated ceramics using TRIM.

A significant source of error (or at least discrepancies between TRIM results from one researcher to the next) is the threshold displacement energies entered by the user for the target material. For

Table 1. SiC Amorphization Threshold Dose at Room Temperature

Ion	Energy (MeV)	Calculated Threshold Dose (dpa)		
		TRIM-92 [4]	TRIM-98	TRIM-2003
N	0.062	0.1	0.13	in progress
Cr	0.260	0.13	~0.18	
H	0.080	0.21	0.31	
N	0.075	0.19	0.25	
Al	0.150	0.26	0.25	
Al	0.130	0.58	0.30	
Si	0.087	0.45	0.36	
Al	0.090	0.28	0.46	
Cl	1.8	≥0.4	~0.6	
He	1.0	~0.6	~1.2	
Fe	3.6	0.5	0.9	
Si	0.56	>0.25	>0.27	

SiC, the consensus displacement energy for Si has varied from 93 eV to 30 eV over the past decade, effectively eliminating any usefulness in comparing current results with past TRIM studies without recalculating (assuming sufficient experimental details are supplied) the previous damage profiles. Fortunately, the consensus displacement energies seem to have settled at 20 eV for C and 35 eV for Si for SiC [5]. It is still up to the individual user to correctly input threshold displacement energies, as well as the target density and other input parameters, because TRIM's defaults are often inappropriate.

The code and stopping powers have improved significantly over the past decade [3, 6], but the results using TRIM's "Quick" Kinchin-Pease calculation method still differ significantly from TRIM's "Full Cascades" Monte Carlo results. Surprisingly, the Kinchin-Pease estimation method generally produces more accurate results than the Monte Carlo method even though the latter requires much more computer runtime. TRIM has been found to produce suspicious results in several cases regardless of which calculation method is used. TRIM calculates far smaller residual vacancy concentrations than the classical Norgett-Robinson-Torrens (NRT) model [7] for light ions at high (~MeV) energies, but results for heavier ions are in better agreement. Detailed energy balance analyses between the energy supplied by the ion beam and the energy dissipated in the target as ionization, phonons and defects show that TRIM fails to account for the entire "input" beam energy, an effect that is seemingly worse for lighter ions than heavier ions.

IRRADIATION-INDUCED CREEP OF MONOLITHIC SIC

Creep capsules have been designed to measure the stress relaxation of monolithic CVD SiC bend bars in response to neutron irradiation. Bend bars, polished and chamfered and having a cross section 1 mm by 1 mm and length of 2 inches, would be inserted into a "rabbit" capsule for irradiation in HFIR to ~5 dpa. The irradiations would be performed at low (~500°C)

temperatures to minimize thermal creep [8]. Each capsule would contain two solid SiC inserts to deflect two SiC bars in a manner analogous to four-point bending (Figure 1). The CVD SiC inserts would expand during irradiation at the same rate as the bend bars, maintaining the radius of curvature and providing uniform heat transfer.

The maximum deflection, y_r, before failure for a bend bar is given by [9]:

$$y_r = \frac{\sigma_o a^2}{4Eh},$$

where y_r is the deflection at the center of the bar, σ_o is the yield stress, a is the distance between the two inner load points, E is the elastic modulus and h is the thickness of the bar (Figure 2). Assuming $\sigma_o = 470$ MPa, $E = 500$ GPa, and $a = 24.4$ mm (0.961") for the 1 mm square SiC bend bars under consideration, the maximum deflection would be only 0.140 mm.

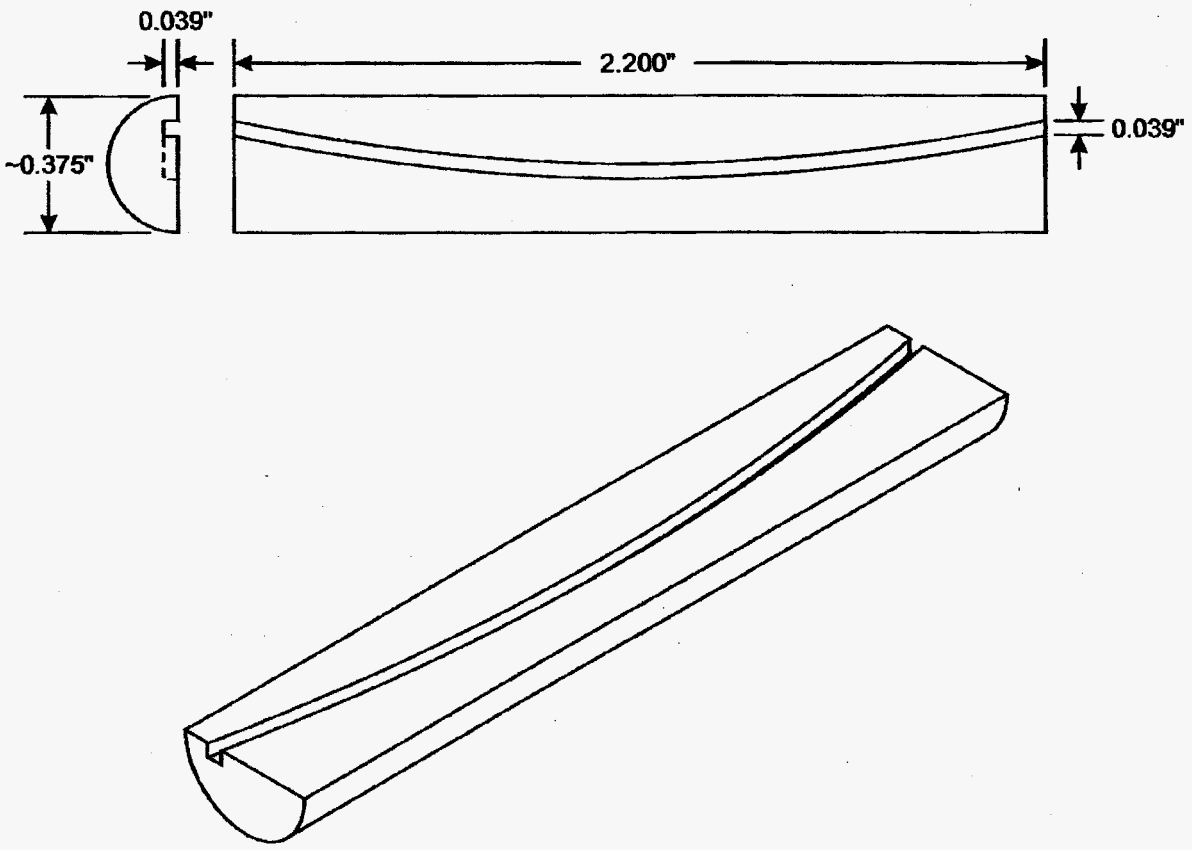

Figure 1. SiC rabbit inserts for bend bar configuration of creep relaxation experiment. Curvature of the bend bar channel is exaggerated to show detail.

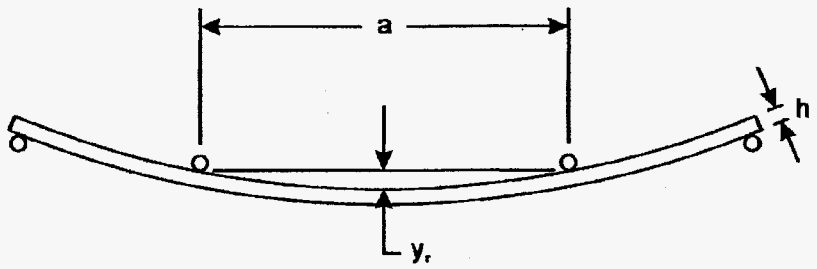

Figure 2. Four point bending parameters.

However, since the rabbit capsule inserts would force a constant radius of curvature over the length of the bend bars, the entire length, l, can be treated as if it were between the two inner loading points in a four point bending rig (Figure 3). In this case, $a \approx 50.8$ mm (2"), and the maximum deflection is 0.607 mm over the entire length. Allowing for a safety factor and loading the bend bars to only half the predicted fracture strain [10] (i.e., $\varepsilon = \frac{1}{2}\frac{\sigma_o}{E}$) reduces the maximum deflection at loading to 0.303 mm. Stress relaxation from this small deflection would prove very difficult to measure, so the bend bar experiment will most likely be replaced by a higher-confidence fiber bend stress relaxation (BSR) experiment [11].

Stoichiometric SCS-9 SiC fiber has recently been obtained, and the 78 μm diameter fiber [12] could be wound around a graphite or vanadium mandrel of approximately the same dimensions as two of the SiC inserts from Figure 1 without difficulty. Fixing the fiber to the mandrel to maintain the radius of curvature during irradiation could be accomplished using alumina cement [13]. The mandrel would have internal space to allow for the concurrent irradiation of temperature monitors and additional specimens. Rabbit design work for this configuration has just begun, but capsules are expected to go into HFIR this summer.

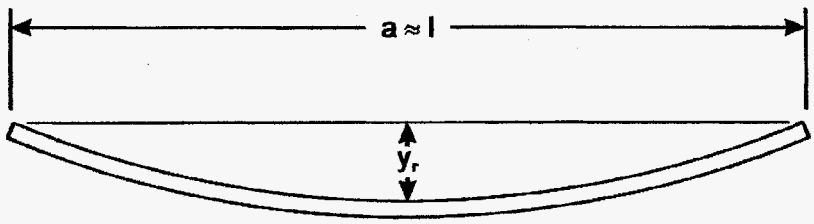

Figure 3. Maximum deflection of bend bar with bending moment applied over entire length.

For either the bend bar or fiber configuration, the post-irradiation analysis is the same. A creep deformation parameter, m, is calculated:

$$m = 1 - \frac{R_o}{R_c},$$

where R_o is the radius of curvature of the fiber segments during irradiation and R_c is the relaxed radius of curvature after irradiation. The irradiation enhanced creep strain, $\Delta\varepsilon_c$ is then given by:

$$\Delta\varepsilon_c = \varepsilon_{avg}\left(\frac{1}{m_{irr}} - \frac{1}{m_{th}}\right),$$

where ε_{avg} is the average bending strain during irradiation [14]. Since irradiation creep dominates the creep behavior of SiC under 1000°C [8], the thermal creep contribution, m_{th}, can be neglected:

$$\Delta\varepsilon_c = \varepsilon_o\left(\frac{1}{m_{irr}} - 1\right).$$

From $\Delta\varepsilon_c$, a creep constant, κ can be calculated:

$$\kappa = \frac{\Delta\varepsilon_c}{\sigma_{avg}(\text{dpa} - \text{rate})}.$$

where σ_{avg} is the average stress applied during irradiation.

METS MELT WIRES

The HFIR Mapping Elevated Temperature Swelling (METS) capsules, containing single crystal and Morton chemical-vapor-deposited (CVD) SiC bend bars (as well as SiC/SiC composite, graphite and alumina bend bars), will be irradiated to ≥4.5 dpa at 780-1650°C. Post-irradiation characterization for the monolithic SiC is expected to include:

- Dimensional change (point defect versus void swelling)
- Elastic modulus
- Hardness
- Indentation fracture toughness
- Thermal diffusivity
- Transmission electron microscopy

Melt wires have been fabricated in support of the METS capsules [15]. Since the METS capsules are uninstrumented, the only method to determine the temperature at which the specimens have been irradiated is to include passive temperature monitors in the capsule.

Table 2. Alloys and Pure Metals Selected for METS Capsule Melt Blocks

Material (wt%)	T_m (°C)
Al	660
Ge	938
18Ni-82Au*	955
Ag	962
7.7Ni-92.3Au	980
5.2Ni-94.8Au	1000
3.5Ni-96.5Au	1020
1.8Ni-98.2Au	1040
Au	1064
Cu	1084
19Pd-81Cu	1100

Material (wt%)	T_m (°C)
39Pd-61Cu	1140
50Pd-50Cu	1180
59Pd-41Cu	1220
60.1Pd-39.9Ni*	1237
49Pd-51Ni	1260
Be	1289
36Pd-64Ni	1300
26Pd-74Ni	1340
17Pd-83Ni	1380
9Pd-91Ni	1420

Material (wt%)	T_m (°C)
Ni	1455
94Pd-6Ni	1475
77Pt-23Ni	
Co	1495
96Pd-4Ni	1500
81Pt-19Ni	
86.5Pt-13.5Ni	1540
Pd	1555
90Pt-10Ni	1580
Pt	1769

* Eutectic composition

Usually, SiC bars with precisely known dimensions are used in capsules to be irradiated to low doses within SiC's point defect swelling temperature regime (<1000°C). Post-irradiation annealing of the SiC over a range of temperatures anneals out the point defects and associated swelling at the irradiation temperature experienced by the capsule at the end of the irradiation [16-21]. The elevated temperatures of most segments of the METS capsules preclude the exclusive use of SiC temperature monitors, so melt wires with melting temperatures spanning the expected maximum temperatures have been created. Visual and radiographic inspection of the wires in a hot cell after irradiation will indicate the maximum irradiation temperature of each capsule segment.

Alloys and pure metals were selected with melting temperatures in the range of 660-1769°C (Table 2). Preference was given in alloy selection to binary systems with minimal (~20°C) temperature gaps between their solidus and liquidus phase diagram lines and with low constituent vapor pressures (<0.0003 Pa at 1100°C). For the purposes of this work, the liquidus temperature for non-eutectic alloy compositions was treated as the melting temperature and this has not presented a problem in visually assessing melting in post-fabrication melting tests. Of the alloy components, only Ni and Pt met the vapor pressure criteria, and significant evaporation was observed in a vacuum ($<8.0 \times 10^{-6}$ torr) for melts containing other elements. No significant melt evaporation has been observed in an environment similar to the internal environment of the METS capsules, static Ar gas at a slight positive pressure (~1 psi at room temperature, increasing to ~7 psi at 1600°C). Therefore, fabrication and melting temperature verification were conducted in Ar.

Fabrication of the alloyed melt blocks was straightforward. The appropriate amounts of each metal were melted together in an alumina crucible at ~90°C above the greater melting temperature of the two components for 40 minutes to produce an ingot ~0.25 cm^3 in volume. Each ingot was compressed to ~1.1 mm thick between two SiC platens at 65 kips in an Instron test machine at a crosshead speed of 0.001-0.005 in/min. The resulting disks were sectioned with a low speed diamond saw to form blocks with the dimensions ~1.1 mm × ~1.5 mm × ~2.0 mm.

Scanning electron microscopy was used to inspect selected alloyed melt blocks for phase separation. Series of melt blocks were "calibrated" in graphite holders over a range of temperatures in ~20°C increments for 1-3 hours per increment to ensure melting at the assumed temperatures. A Type-S thermocouple and an optical pyrometer were used to verify the temperatures. Melting was visually assessed after each temperature interval.

The alloys in Table 2 were selected to avoid the formation of secondary phases, and no secondary phases have been observed. Several melt blocks were annealed at 100°C below their melting points for up to 6 hours to improve their homogeneity, but calibration has shown no difference in melting temperature between as-fabricated and annealed melt blocks.

Each of the three METS capsules contains ten subcapsules, and each subcapsule has been designed to accommodate a graphite holder for melt blocks at each end, top and bottom. Up to eight melt blocks and up to three SiC temperature monitors will be sealed in each graphite holder, selected according to the calculated maximum temperature to be experienced within the subcapsule (Table 3). Post-irradiation visual and/or radiographic inspection of the holders in a hot cell should show that some, but not all, of the blocks in each holder have melted, indicating the maximum temperature reached (to within ~20°C in most cases). For the lower temperature subcapsules, annealing and dimensional analysis of SiC temperature monitors will provide a supplemental estimate of the temperature at the end of irradiation with an accuracy of ~±30-45°C [20, 21].

Table 3. METS Capsule Melt Block Loading List

Sub-capsule	T (°C) Range	Posi-tion	T_m of Selected Melt Blocks (°C)							
1	780-860	top	SiC*	SiC*	SiC*	660	938	955	962	
		bottom	SiC*	SiC*	SiC*	660	938	955	962	
10	790-920	top	SiC*	660	938	955	962	980	1000	1020
		bottom	SiC*	660	938	955	962	980	1000	1020
3	820-1100	top	SiC*	938	962	1000	1020	1084	1140	1220
		bottom	SiC*	938	980	1040	1064	1100	1180	1220
2	850-1000	top	SiC*	938	955	962	1000	1020	1064	1100
		bottom	SiC*	938	962	980	1000	1040	1084	1100
9	920-1075	top	SiC*	938	955	980	1020	1064	1100	1180
		bottom	SiC*	938	962	1000	1040	1084	1140	1180
8	1030-1200	top	938	980	1020	1064	1100	1180	1237	1300
		bottom	938	1000	1040	1084	1140	1220	1260	1300
4	1150-1290	top	1040	1084	1140	1180	1237	1289	1340	1420
		bottom	1040	1100	1140	1220	1260	1300	1380	1420
7	1290-1390	top	1180	1220	1289	1340	1380	1420	1455	1495
		bottom	1180	1260	1300	1340	1380	1420	1475	1495
5	1440-1540	top	1340	1380	1455	1475	1500	1555	1580	1769
		bottom	1340	1420	1455	1495	1540	1555	1580	1769
6	1520-1650	top	1420	1455	1475	1495	1540	1555	1580	1769
		bottom	1420	1455	1475	1500	1540	1555	1580	1769

*SiC temperature monitor [14-19]

HERMETICITY OF SIC/SIC COMPOSITES

Composite tubes 1.5 inches in diameter and 4 inches in length were fabricated from plain Nicalon™ (Nippon carbon) cloth and infiltrated with SiC by forced flow CVI. Following processing, the composite tubes were machined into a cylindrical "dog bone" geometry with a gage section 2.2 inches in length and a wall thickness of 0.25 inches. Figure 4 shows the gross gas permeability of one of the CVI SiC/SiC specimens before PIP. The gage sections of the machined tubes were infiltrated with a polymeric solution of 2.5% allyl-hydridopolycarbosilane (HPCS) that was pyrolyzed into stoichiometric SiC. HPCS infiltration and pyrolysis were repeated for 12 to 18 cycles until the helium permeation rate through the wall of each gage section was less than 2×10^{-5} mol m^{-2} s^{-1} at room temperature and 1 atm upstream pressure [22].

The geometry of the specimens has proven somewhat unsuitable for tensile testing, causing failure at the specimen grips instead of in the gage section. Figure 5 shows the stress-displacement curve for a Nicalon/SiC composite tube of the same geometry without HPCS infiltration. The tube failed at the Instron tensile machine grips at 100 MPa instead of the expected 200 MPa [1]. Every effort to eliminate off-axis stresses has been made, including fabrication and testing of graphite specimen replicas, without success. Further machining of the HPCS-infiltrated SiC/SiC specimens is undesirable because any reduction in wall thickness to induce failure along the gage section would have a detrimental effect on hermeticity. The HPCS-infiltrated specimens have less porosity than the plain CVI tube of Figure 4, and some progress has been made in fixturing and aligning the tensile machine grips to reduce off-axis stresses, so it is expected that the HPCS-infiltrated tubes will exhibit greater ultimate tensile strengths and significant matrix microcracking and corresponding loss of hermeticity along the gage length even if failure occurs at the tensile machine grips.

The HPCS-infiltrated SiC/SiC composite tubes will therefore be tensile tested while measuring helium leakage and acoustic emissions. Helium permeability as a function of applied stress is necessary design data for potential fusion devices, and very limited study has been conducted to date in this area. The recorded acoustic emissions will be used to correlate composite failure events (matrix microcracking and fiber breakage) with changes in leak rates, providing insight into the evolution of flow paths through the composite structure.

Figure 4. Argon permeability of CVI Nicalon/SiC tube at only 5 psi internal pressure prior to HPCS infiltration.

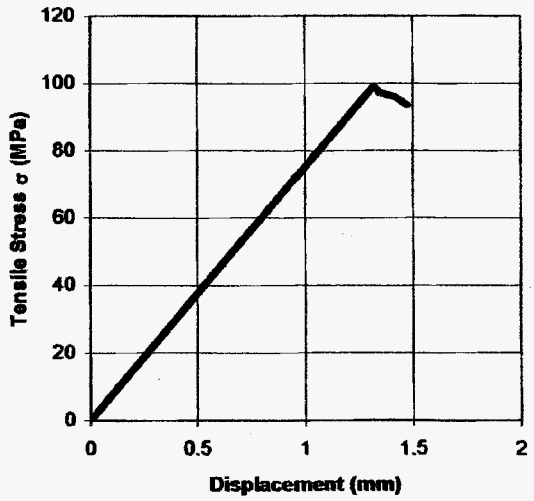

Figure 5. Failure curve for CVI Nicalon/SiC tube with the same geometry as the HPCS-infiltrated hermeticity specimens. Failure occurred at the tensile machine grips at one half the expected ultimate tensile strength.

FUTURE WORK

Research in the areas of TRIM computer code modeling of radiation damage in SiC, irradiation-induced creep of SiC, and elevated temperature response of SiC to irradiation will be incorporated into a dissertation entitled, *An Assessment of Several Issues Affecting the Feasibility of SiC/SiC Composites as Structural Materials for Fusion Applications*, expected to be completed by the summer of 2004. The hermeticity study is not directly related to operating temperature and will be included in other publications. Activities to be accomplished during the coming year are described below.

Computer Modeling of Radiation Damage in SiC

TRIM-2003 case runs comparing damage profiles to experimental results from ORNL researchers and the literature are in progress. Runs comparing the results of differing input parameters and TRIM calculation methods for the same cases are also continuing. Sufficient output has been generated and analyzed to warrant a *Nuclear Instruments and Methods B* paper on the caveats of using TRIM to calculate damage profiles for the various ion beam experiments conducted by the fusion community. A new edition of the authors' tutorial book [23] detailing TRIM's calculation methods is due to be published in 2003 and will be reviewed for relevant insights if time permits.

Irradiation-Induced Creep of Monolithic SiC

HFIR creep capsule "rabbits" should be fabricated and inserted into HFIR by the middle of 2003. Current intentions are to employ the fiber bend stress relaxation (BSR) technique rather than the previously contemplated bend bar configuration. At least two different irradiation doses (to be determined) are planned for the HFIR rabbits; capsules should be pulled from HFIR in late 2003 and early 2004, and analyses should be completed by the middle of 2004.

Mapping Elevated Temperature Swelling of SiC

Melt wires for the HFIR METS experiment have been fabricated. Some further melting temperature verification of the melt wires in a conventional furnace is still desirable and is pending an argon gas feed to the furnace. Capsule completion and insertion into HFIR still require HFIR's approval of the specimen loading list and completion of the trefoil holder enabling adequate cooling. It is anticipated that the capsules will be completed by June with irradiation commencing shortly thereafter. Specimens should start being available for analysis in late 2003.

Hermeticity of SiC/SiC Composites

Because of the recent decision to abandon attempts to force gross failure in the gage sections of the HPCS-infiltrated SiC/SiC specimens, relying instead on the data gained as hermeticity

degrades due to matrix microcracking along the gage sections, the specimens are ready to be broken, pending equipment availability.

References

[1] A. Hasegawa, A. Kohyama, R. H. Jones, L. L. Snead, B. Riccardi and P. Fenici, J. Nucl. Mater. 283-287 (2000) 128.
[2] J. P. Biersack and L. G. Haggman, Nucl. Instrum. and Meth. 174 (1980) 93.
[3] J. F. Ziegler, Particle Interactions with Matter, http://www.srim.org, 2003.
[4] L. L. Snead and S. J. Zinkle, in Microstructure of Irradiated Materials, MRS Symposium Proceedings vol. 373, eds. I. M. Robertson et al. (Materials Research Society, Pittsburgh, 1995) 377.
[5] H. L. Heinisch, in Fusion Mater. Semiann. Prog. Rep. for Period Ending June 30, 1998, DOE/ER-0313/24 (ORNL, 1998).
[6] J. F. Ziegler, J. Appl. Phys. / Rev. Appl. Phys. 85 (1999) 1249.
[7] M. J. Norgett, M. T. Robinson and I. M. Torrens, Nucl. Eng. and Design 33 (1975) 50.
[8] A. El-Azab and N. M. Ghoniem, Fusion Tech. 26 (1994) 1250.
[9] G. W. Hollenberg, G. R. Terwilliger and R. S. Gordon, J. Am. Ceram. Soc. 54 (4) (1971) 196.
[10] R. J. Price, Nucl. Tech. 35 (1977) 320.
[11] G. N. Morscher and J. A. DiCarlo, J. Am. Ceram. Soc. 75 (1) (1992) 136.
[12] Specialty Materials, Inc., SCS Silicon Carbide Fibers, http://www.specmaterials.com/silicarbsite.htm, 2003.
[13] R. Scholz and G. E. Youngblood, J. Nucl. Mater. 283-287 (2000) 372.
[14] G. E. Youngblood, R. H. Jones, G. N. Morscher, R. Scholz and A. Kohyama, Eng. Sci. Proc. 19 (4) (1998) 341.
[15] S. D. Connery, L. L. Snead and D. Steiner, in Fusion Mater. Semiann. Prog. Rep. for Period Ending June 30, 2000, DOE/ER-0313/28 (ORNL, 2000).
[16] N. F. Pravdyuk, V. A. Nicolaenco, V. I. Karpuchin and V. K. Kusnetosov, in Property of Reactor Materials and the Effect of Radiation Damage, ed. D. J. Littler (Butterworths, London, 1962) 57.
[17] R. P. Thorne and V. C. Howard, Proc. Brit. Cer. Soc. 7 (1967) 439.
[18] J. I. Bramman, A. S. Fraser and W. H. Martin, J. Nucl. Energy 25 (1971) 223.
[19] R. J. Price, Nucl. Tech. 16 (1972) 536.
[20] J. E. Palentine, J. Nucl. Mater. 61 (1976) 243.
[21] J. E. Palentine, J. Nucl. Mater. 92 (1980) 43.
[22] S. D. Connery, L. L. Snead, and D. Steiner, presented at 9th Int. Conf. on Fusion Reactor Materials, Colorado Springs, CO, USA, Oct. 1999.
[23] J. F. Ziegler, J. P. Biersack and U. Littmark, The Stopping and Range of Ions in Solids (Pergamon Press, New York, 1985).